Geologia Croatica	57/2	149–158	7 Figs.	2 Tabs.		ZAGREB 2004

Microstructures in Two Alkali Feldspar Megacrysts from the Papuk Mt., Croatia

Viktória **KOVÁCS KIS**[1], Marija **HORVAT**[2] and István **DÓDONY**[1]

Key words: Microstructure, Modulation, Alkali feldspar, Low microcline, Thermal history, Papuk Mt., Croatia.

Abstract

Two types of megacrysts, one from Pakra Creek and the other from the Sloboština Creek locality proved to be low microcline in association with low albite and quartz. A sample from Pakra Creek is a vein filling megacryst characterised by the absence of twinning. The deduced crystallization temperature is below 460°C. The sample from Sloboština Creek is a pocket forming megacryst which shows tweed-like texture, with deduced crystallization temperature near to but above 460°C. Both samples are characterized by a continuously modulated lattice on the submicroscopic scale.

1. INTRODUCTION

The Papuk Mt. belongs to the Slavonian Mountains in Croatia. It is situated in the southernmost part of the Tisza Megaunit (Fig. 1). Comprehensive reviews of the geological setting of this area are given by JAMIČIĆ & BRKIĆ (1987), JAMIČIĆ (1989) and KOROLIJA & JAMIČIĆ (1989). VRAGOVIĆ (1965) gave a detailed petrographic description of the gneisses, granitoids and the pegmatites of this region. Based on geochemical and isotope data PAMIĆ & LANPHERE (1991) and PAMIĆ et al. (1996) grouped granitoids occurring in the Slavonian Mountains to the Hercynian S-type and I-type group.

KUČAN & KRMPOTIĆ (1911) reported the first alkali feldspar megacrysts from the Papuk Mt. (Pakra Creek). They studied the megacrysts under a petrographic microscope and described them as "microcline-microperthites" in a gneiss host. TAJDER (1957) mentioned "large-sized pink microcline" crystals occurring in pegmatitic pockets (Sloboština Creek) and veins in granitoids (Pakra Creek). VRAGOVIĆ (1965) differentiated megacrysts based on their colours and occurrence in the host as porphyric (in adamellite and granodiorite), vein filling and diffuse, metasomatic K-feldspar megacrysts.

The Al–Si ordering and microstructures provide evidence for the thermal history of feldspars. The features of alkali feldspars crystallised from a melt have been well studied. There are three important processes that occur in feldspar crystals during cooling (McCONNELL, 1969; EGGLETON & BUSECK, 1980; McLAREN, 1984; SALJE & KUSCHOLKE, 1984; BROWN & PARSONS, 1988; SMITH & BROWN, 1988; McCONNELL et al., 1997): (1) the homogenous composition disproportionates (exsolutes) into K- and Na-rich lamellae and lenses at high temperature; (2) the C2/m symmetry degrades to $C\bar{1}$; (3) albite and microcline twinning occur in both Na- and K-rich lamellae, respectively. The last two processes are simultaneous. The microstructural features, i.e. the size distribution and the orientation of the K- and Na-rich domains, the density of twinning and transitional state between the C2/m and $C\bar{1}$ symmetries reflect the crystallization conditions. WILLAIME et al. (1976) produced a complete list of alkali-feldspar microstructures depending on the melt composition and cooling rate.

The microstructures of alkali feldspars crystallised at lower temperatures are relatively less known. TEM observations of twinning and exsolution texture in a hydrothermal and two pegmatitic microclines (TIBBALS & OLSEN, 1977) extended the study of K-feldspar microtextures below the temperature of the monoclinic–triclinic transformation. K-metasomatism and the formation of microcline under 0.4–1.5 kbar and 250–450ºC in hydrothermal quartz-depleted granites of European granite massifs were investigated by CATHELINEAU (1986). WHITE & BARNETT (1990) studied untwinned low-microcline grains from the Hemlo gold deposit, Ontario, which formed below the monoclinic–triclinic transformation. Authigenic K-feldspar derived from potassium-rich volcanic ash (HAYNES, 1994), is characterised by compositional purity and a lack of zoning and twinning.

The goal of this paper is to characterise the microstructure of alkali feldspar megacrysts and give evidence for their origin. Since the submicron scale mineralogy of the abundant alkali feldspar megacrysts from the Papuk Mt. was unknown this paper provides

[1] Department of Mineralogy, Eötvös L. University, Pázmány Péter sétány 1/c, H-1117 Budapest, Hungary;
e-mail: vis@geology.elte.hu

[2] Institute of Geology, Sachsova 2, HR-10000 Zagreb, Croatia.

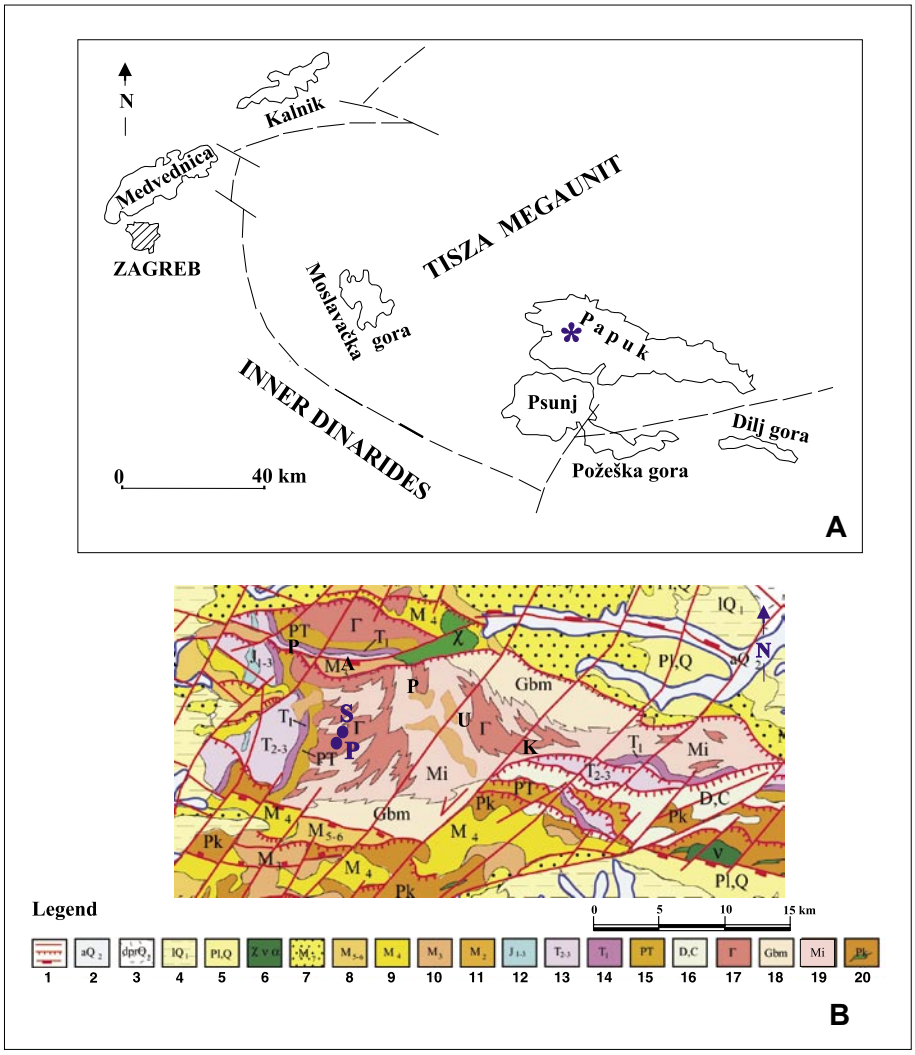

Fig. 1 (A) Tectonic scheme of the basement in the SW part of the Pannonian basin (after ŠIKIĆ, 1995). Asterisk shows the position of the investigated area. (B) Part of the compiled geological map of the Slavonian Mts. (JAMIČIĆ, 2001) with sampling localities (P – Pakra, S – Sloboština Creek). Legend: 1) main tectonic lines; 2) alluvium of creeks; 3) deluvial–proluvial deposits; 4) loess; 5) Pliocene–Quaternary: gravel and sands; 6) albite rhyolite, andesite, basalt; 7) Pontian: sand, marl and clay; 8) Sarmatian–Pannonian: marl and limestone; 9) Badenian: conglomerate, limestone, marl; 10) Carpathian: conglomerate, sand, clay and marl; 11) Ottnangian: conglomerate, sand, gravel; 12) Jurassic: limestone; 13) Middle and Upper Triassic: dolomite, dolomitic limestone; 14) Lower Triassic: sandstone, siltstone, shale; 15) Permotriassic: quartz sandstone, conglomerate; 16) Devonian–Carboniferous: graphitic schist, conglomerate, sandstone; 17) granitoids; 18) gneiss; 19) migmatite; 20) chlorite–sericite schist, metagabbro, marble, amphibolite, amphibole schist; phlaseride granitoid, garnet–staurolite gneiss.

the first description and genetic interpretation of their microstructure.

2. SAMPLES AND EXPERIMENTAL METHODS

Megacrysts were collected at two localities: Pakra Creek valley (P) and Sloboština Creek valley (S) (Fig. 1B). Pakra Creek megacrysts are pink and they were found in a 10 cm wide vein, which crosses the porphyric granitoid body. Sloboština Creek megacrysts are pale, greyish pink and they are from a 40 cm sized pocket occurring in the migmatite. Their size is about 5 x 3 x 1.5 cm. The K-feldspar megacrysts contain crystalline inclusions of plagioclase and quartz. The host rock is coarse grained where the alkali feldspars have the largest size.

The chemical and structural inhomogeneities of the megacrysts were measured using a polarizing microscope, a scanning microscope for electron probe microanalysis (EPMA) and a transmission electron microscope (TEM).

The modal composition was determined using a polarizing microscope equipped with an ocular net. The value of standard deviations of repeated measurements was below 4%.

Quantitative chemical analyses were carried out on a JEOL JCXA–733 wavelength dispersive (WDS) electron microprobe equipped with three spectrometers operating at 15 kV and 36 nA, using ZAF correction. The following standards were applied: albite for Si, Al and Na, wollastonite for Ca and orthoclase for K.

The X-ray powder diffraction (XRPD) measurements were performed on a SIEMENS D500 powder diffractometer (Cu radiation, 40kV, 20 mA, analogous registration at 0.5° 2θ/min goniometer speed). For the d-value measurements the reflections of accompanying quartz (JCPDS #33–1161) were used as an inner standard.

The samples for TEM observations were obtained by grinding the sample under ethanol and mounting a drop from suspension onto a Cu-grid covered by amorphous carbon supporting film. The selected area electron diffraction (SAED) patterns and the images were

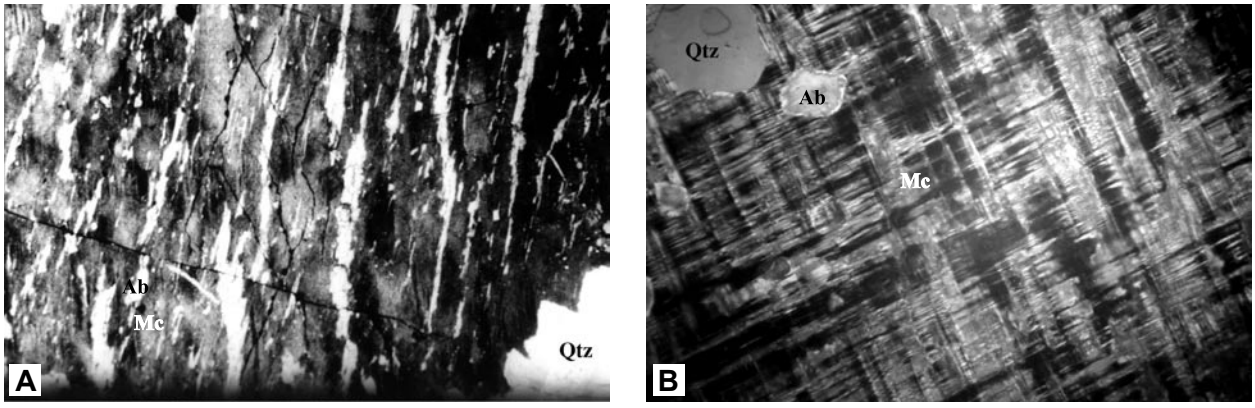

Fig. 2 Micrographs of alkali feldspar megacrysts. Cross-polarised light, the width of the photographs are 1.3 mm. (A) Na-feldspar patches in microcline host with no cross-hatched extinction pattern of microcline (Pakra Creek). (B) Cross-hatched extinction pattern of microcline (Sloboština Creek). Legend: Ab – Na feldspar patches; Mc – microcline; Qtz – quartz.

obtained with a JEOL JEM 100U microscope operating on 100 kV.

3. RESULTS

Under a petrographic microscope, the Pakra Creek megacryst shows an inhomogeneous texture, where 10–50 μm sized albite patches form layers in microcline. The extinction of albite patches can be regarded as simultaneous, whereas microcline shows inhomogeneous undulatory extinction (Fig. 2A). No twins were observed in this sample. Besides the randomly distributed feldspar components, isometric quartz grains also occur. The result of the modal analysis is microcline 82%, albite 15% and quartz 3%.

The Sloboština Creek sample is different to that of Pakra Creek. The size of the albite patches are about 10 μm, with rather isometric or tabular forms. Quartz shows no graphic texture, but the host microcline shows a cross-hatched extinction pattern (Fig. 2B). The result of the modal analysis is microcline 88%, albite 9% and quartz 3%.

Elemental analyses were made at several points in the potassium and sodium rich regions. The composition ranges between $Or_{91-96}Ab_{8-4}An_{0-4}$ and $Ab_{99-97}Or_{0-1}An_{0-2}$ respectively (Table 1). Figure 3 shows the measured area of the Pakra Creek megacryst (A) and back-scattered image of potassium distribution (B).

Besides minor quartz, the samples proved to be microcline on the basis of their XRPD patterns. Both samples show splitted {131} potassic feldspar reflections in their patterns, which prove their triclinic symmetry which is characteristic for microcline. Using the calculation introduced by GOLDSCHMIDT & LAVES (1954) the value of triclinicity ($\Delta=(d_{(131)}-d_{(1\bar{3}1)})*12.5$) is 0.93 and 0.81 for the Pakra Creek and Sloboština Creek samples, respectively. Using a complex evaluation system method published by NEVES & GODINHO (1995, 1999), index of order $\Delta_{SM}=15.32-[2\theta_{(\bar{2}04)}-2\theta_{(060)}]/0.608$ is 0.98 and 0.91 for Pakra and Sloboština Creek megacrysts, respectively. The [110] method (KROLL & RIBBE, 1983) was used for determining the structural state of some K-feldspars from different rock types in the Papuk area, as a measure of the Al/Si

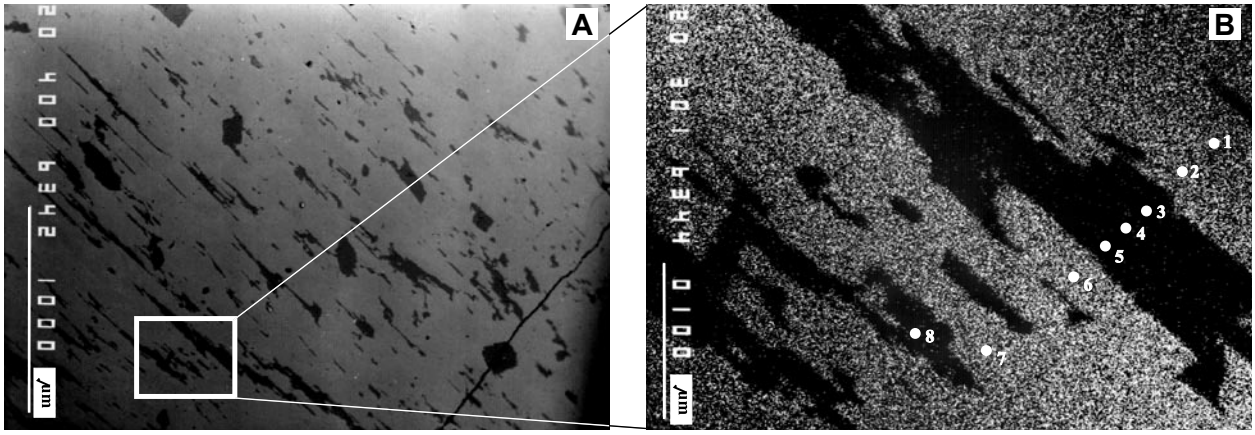

Fig. 3 Measured area of Pakra Creek megacrysts (A). Back-scattered electron image – potassium-map (B) with measuring points numbered from 1 to 8 (see Table 1).

	Measured areas of the Pakra Creek sample												
	1	**2**	**3**	**4**	**5**	**6**	**7**	**8**	**9**	**10**	**11**	**12**	**13**
							wt%						
SiO_2	64.38	63.61	67.65	67.79	68.29	63.89	64.01	67.81	67.8	67.59	67.99	64.06	64.75
Al_2O_3	18.70	18.66	19.81	19.63	19.39	18.21	18.57	20.13	19.79	19.80	19.89	18.70	18.65
CaO	0.05	0	0.45	0.08	0.14	0.76	0.02	0.48	0.25	0.20	0.27	0	0
Na_2O	0.78	0.50	11.17	11.44	11.27	0.57	0.55	11.22	11.44	11.35	11.26	0.58	0.93
K_2O	15.94	16.27	0.13	0.19	0.11	15.75	16.16	0.14	0.17	0.14	0.15	16.04	15.57
Σ	**99.85**	**99.04**	**99.21**	**99.13**	**99.20**	**99.18**	**99.31**	**99.78**	**99.45**	**99.08**	**99.56**	**99.38**	**99.90**
							Number of ions on the basis of 8 (O)						
Si	2.980	2.975	2.978	2.987	3.002	2.982	2.982	2.970	2.979	2.979	2.981	2.980	2.989
Al	1.021	1.029	1.028	1.020	1.005	1.002	1.020	1.039	1.025	1.029	1.028	1.025	1.015
Ca	0.002	0.000	0.021	0.004	0.007	0.038	0.001	0.023	0.012	0.009	0.013	0	0
Na	0.070	0.045	0.952	0.976	0.959	0.052	0.050	0.952	0.974	0.969	0.956	0.052	0.083
K	0.942	0.971	0.007	0.011	0.006	0.938	0.961	0.008	0.010	0.008	0.008	0.952	0.917
							mol %						
An	0.2	0.0	2.2	0.4	0.7	3.7	0.1	2.3	1.2	1.0	1.3	0	0
Ab	6.9	4.5	97.1	98.5	98.7	5.0	4.9	96.9	97.8	98.2	97.8	5.2	8.3
Or	92.9	95.5	0.7	1.1	0.6	91.3	95.0	0.8	1.0	0.8	0.9	94.8	91.7

	Measured areas of the Sloboština Creek sample							
	1	**2**	**3**	**4**	**5**	**6**	**7**	**8**
				wt%				
SiO_2	64.40	64.13	67.26	67.73	67.63	68.20	64.43	64.10
Al_2O_3	18.74	18.64	19.79	19.81	19.74	19.55	18.61	18.61
CaO	0	0.02	0.25	0.36	0.35	0.13	0.01	0
Na_2O	0.46	0.93	11.40	11.29	11.26	11.44	0.64	0.40
K_2O	16.36	15.56	0.09	0.11	0.09	0.07	15.91	16.16
Σ	**99.96**	**99.28**	**98.79**	**99.30**	**99.07**	**99.39**	**99.60**	**99.27**
				Number of ions on the basis of 8 (O)				
Si	2.981	2.982	2.975	2.979	2.981	2.994	2.987	2.985
Al	1.023	1.022	1.032	1.027	1.026	1.012	1.017	1.022
Ca	0	0.001	0.012	0.017	0.017	0.006	0	0
Na	0.041	0.084	0.976	0.962	0.961	0.973	0.057	0.036
K	0.966	0.923	0.005	0.006	0.005	0.004	0.941	0.960
				mol %				
An	0.0	0.1	1.2	1.7	1.7	0.6	0.0	0.0
Ab	4.1	8.3	98.3	97.7	97.8	99.0	5.7	3.6
Or	95.9	91.6	0.5	0.6	0.5	0.4	94.3	96.4

Table 1 Chemical data of the studied feldspar crystals. The measured areas of the Pakra Creek sample are numbered in Fig. 3B. An, Ab and Or stands for $CaAl_2Si_2O_8$, $NaAlSi_3O_8$ and $KAlSi_3O_8$ content, respectively.

distribution among the non-equivalent tetrahedral sites (LOVAS et al., 1999). [110] and [1$\bar{1}$0] translation, calculated from unit cell parameters and unit cell volume obtained by Rietveld refinement, gave an Al content in t_1o site 0.9847 and 0.9806, for the Pakra and Sloboština Creek megacrysts, respectively. Among the microcline reflections of the Pakra Creek sample, low albite peaks appear separately at the following d-values: 4.02 Å, 3.77 Å, 3.66 Å, 3.19 Å, 2.86 Å and 2.62 Å (Table 2). Besides similar low albite reflections, an additional low albite reflection (d=2.93 Å) appears in the XRPD pattern of Sloboština Creek sample.

The transmission electron microscopy allows us to study the structural properties of individual potassium and sodium rich regions. Figure 4 is a [100] SAED pattern of the feldspar crystal from Sloboština Creek. The angle between $\mathbf{b}^*$ and $\mathbf{c}^*$ vectors equals 90º, so the crystal seems to be monoclinic.

On the basis of the ICSD database (BERNDT, 1995) the value of $\mathbf{b}^*/\mathbf{c}^*$ ratio for potassic feldspars reaches

d_{ob} (Å) Pakra sample	d_{ob} (Å) Sloboština sample	$I_{relative}$ Pakra sample	$I_{relative}$ Sloboština sample	mineral	d_{lit} (Å)	hkl	I_{lit}
6.7223	6.7478	0.8	0.6	max microcline	6.736	110	5
6.4775	6.4822	5.5	5	max microcline	6.477	020	5
	6.4168		2	low albite	6.376	020	9
5.9217	5.9653	0.6	0.5	max microcline	5.923	$\bar{1}\bar{1}1$	4
5.8211	5.8594	0.3	0.3	max microcline	5.8	$\bar{1}11$	3
4.6059	4.6201	0.5	0.4	max microcline	4.603	021	3
4.2183	4.2322	5.7	3.9	max microcline	4.213	$\bar{2}01$	51
4.0239	4.0401	2.1	1	low albite	4.027	$\bar{2}01$	61
3.9776	3.9882	4.1	2.6	max microcline	3.984	111	12
3.9273	3.9428	0.9	0.7	max microcline	3.924	$1\bar{1}1$	6
3.8257	3.8403	4.5	3.1	max microcline	3.831	130	30
3.7760	3.7903	1.5	1.9	low albite	3.777	111	26
3.7063	3.7231	3.6	2.4	max microcline	3.704	$\bar{1}30$	30
3.6612	3.6701	1.9	1.8	low albite	3.658	$\bar{1}30$	34
3.6043	3.6043	0.8	0.7	max microcline	3.595	$\bar{2}\bar{2}1$	9
3.4809	3.4796	7.3	5.8	max microcline	3.484	$\bar{1}12$	29
3.3674	3.3759	10.4	5.2	max microcline	3.368	220	41
3.2962	3.2903	7.1	5.3	max microcline	3.286	$\bar{2}02$	48
3.2491	3.2445	100	100	max microcline	3.246	002	100
3.1966	3.1988	9.4	15.7	low albite	3.188	040	100
3.0308	3.0278	5	2	max microcline	3.033	131	19
2.9563	2.9631	4.8	2.6	max microcline	2.958	$1\bar{3}1$	26
	2.9374		0.5	low albite	2.928	$0\bar{4}1$	19
2.9057	2.9048	4.3	3.8	max microcline	2.906	041	17
2.8648	2.8720	0.3	0.4	low albite	2.862	131	9
2.7866	2.7900	1.4	0.8	max microcline	2.782	$\bar{1}\bar{3}2$	7
2.6225	2.6232	2.1	1.4	low albite	2.637	$\bar{1}32$	7
2.5679	2.5729	2.5	1.9	max microcline	2.570	112	8
2.5397	2.5286	1.2	1.3	max microcline	2.536	310	5
2.5252		1.7		max microcline	2.525	240	15
2.4314	2.4352	1.3	0.9	max microcline	2.432	$\bar{1}\bar{5}1$	6
2.3939		0.3		max microcline	2.389	$\bar{1}51$	2
2.3359	2.3382	1.7	1.4	max microcline	2.334	$\bar{1}\bar{1}3$	7
2.2819	2.2846	0.4	0.4	max microcline	2.296	$\bar{3}\bar{3}2$	2
2.2288		0.4		max microcline	2.226	$\bar{3}32$	2
2.1600	2.1614	6.8	4.9	max microcline	2.16	241	21
2.1179		0.7		max microcline	2.113	$\bar{4}01$	3
2.0785	2.0808	0.8	0.6	max microcline	2.078	311	3
1.9926	1.9926	1.9	1.1	max microcline	1.992	222	5
1.9633	1.9669	7.6	0.6	max microcline	1.974	$\bar{3}\bar{3}3$	5
1.9275	1.9286	1.0	0.6	max microcline	1.925	400	8
1.9160	1.9148	0.7	0.4	max microcline	1.911	331	5
1.8923	1.8916	0.3	0.4	max microcline	1.892	$\bar{2}61$	1
1.8647	1.8611	1.7	1.4	max microcline	1.866	113	4
1.8210	1.8217	1.2	0.6	low albite	1.820	400	9
1.8059	1.8055	5.1	4.1	max microcline	1.806	043	20

Table 2 XRPD data sets of the investigated samples, low albite (JCPDS number 20–0554) and maximum microcline (JCPDS number 22–0687).

value of 2 in the Al/Si ordering between orthoclase and microcline. The value of $d_{(020)}/d_{(002)}$ in [100] SAED pattern (Fig. 4) was measured on a digitised image (resolution=510 dpi, K=1024 dot*Å) and the result is exactly 2. This fact, together with the missing odd reflections implicated by the C-centred unit cell, makes the main directions indistinguishable. However, accurate indexing is possible due to disordering parallel to the $\mathbf{b}^*$.

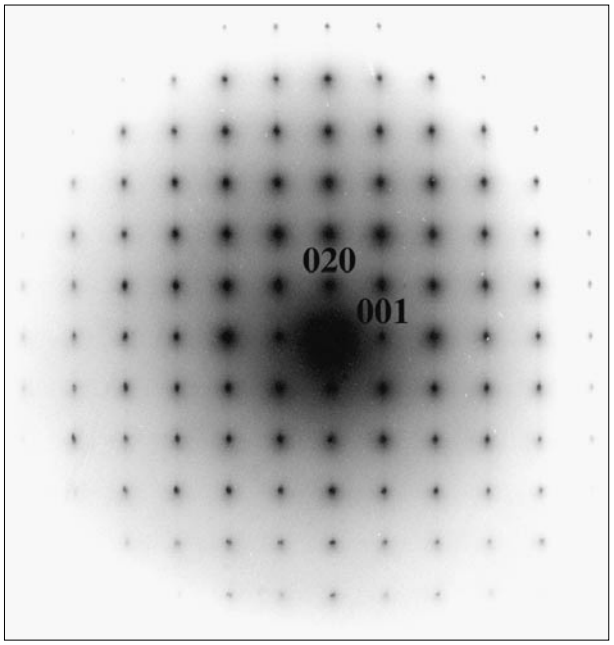

Fig. 4 [100] SAED pattern of a crystallite from the Sloboština Creek sample. Note that the reflections are equidistant in both directions and a slight continuous scattering appears parallel to $\mathbf{b}^*$.

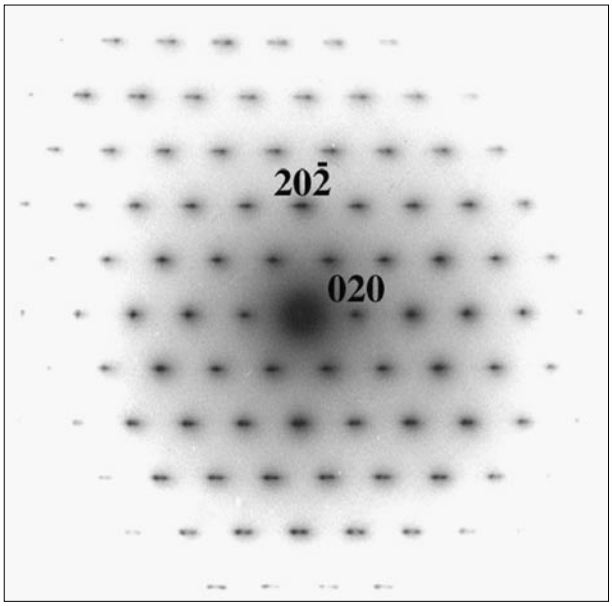

Fig. 5 <$\bar{1}0\bar{1}$> zone SAED pattern of the Pakra Creek sample contains elongated and double reflections.

Streaking parallel to $\mathbf{b}^*$ is also observable on <$\bar{1}0\bar{1}$> zone SAED patterns (Fig. 5). In contrast to the [100] pattern in Fig. 4, here the streaking is not continuous but the individual reflections are separated at higher *hkl* values. However, reflections split parallel to $\mathbf{b}^*$ is reminiscent of the (010) albite twinning; the observed geometry, the measured angles and streaking exclude this interpretation. The albite twinning requires mirror symmetry for doubled reflections, but the <20$\bar{2}$> axes incline to the **b*** with different angles (87.6º and 90.6º, respectively). These angles are close to the same value of the maximum microcline (88.1º, calculated from data of BLASI et al., 1984), and the $d_{(020)}/d_{(20\bar{2})}$ ratio also matches closely with this data.

[1$\bar{1}$0] projection of a Pakra Creek crystallite is seen in Fig. 6A. The measured angle between the $[11\bar{1}]^*$ and $[112]^*$ and d-values ratio in Fig. 6 support microcline and correspond to published data of BLASI et al. (1984). For structural refinement BLASI et al. (1984) used a specimen of maximum microcline which was found as an overgrowth on an amazonitic microcline perthite from a pegmatitic pocket in the Pikes Peak batholith, Colorado, so the specimen can be considered as a close maximum microcline end-member. The shape of reflections is slightly streaked parallel to the $[11\bar{1}]^*$ direction. This suggests that the crystallite tends to order towards the ideal triclinic structure. No continuous streaking nor reflection splitting is observable.

The bright field image (Fig. 6B) of the same crystal shows a tweed-like contrast system. The dense modulation is parallel to the (11$\bar{1}$) planes, where the modulation forms continuous, sometimes terminal or zigzag shaped ribbons and lenses corresponding to the streaking in the SAED pattern (Fig. 6A). The less dense modulation is roughly perpendicular to the (11$\bar{1}$) planes. These dark areas represent very fine Na-rich domains in the host, with bulk composition over 96% $KAlSi_3O_8$ (Table 1). The periodicity of (11$\bar{1}$) modulation is around 0.02 μm.

4. DISCUSSION

Most of the real structural observations of alkali feldspars have been performed on samples crystallised from melts and which underwent solid phase transformations (comprehensive reviews in WILLAIME et al., 1976; RIBBE, 1983; BROWN, 1984; SMITH & BROWN, 1988; GRIFFEN, 1992; DEER et al., 2001). The origin and thermal history of these feldspars have been discussed by several authors (WILLAIME et al., 1976; McLAREN, 1984; XU et al., 2000). Real structures in alkali feldspars formed at lower temperature and from metasomatic, hydrothermal and diagenetic origin have so far been peripheral for TEM studies (e.g. TIBBALS & OLSEN, 1977).

The result of the XRPD analysis – that the main constituent is near maximum microcline – was supported by TEM studies. Besides ordered low microcline, minor low albite occurs in the megacrysts showing a close orientation relationship to the host. The observed textures of albite in a potassic feldspar host reveal, under the polarizing microscope, the formation of both megacrysts with no perthitic exsolution: the grain boundaries do not show crystallographic interrelations (Figs. 2 and 3) and the simultaneous extinction

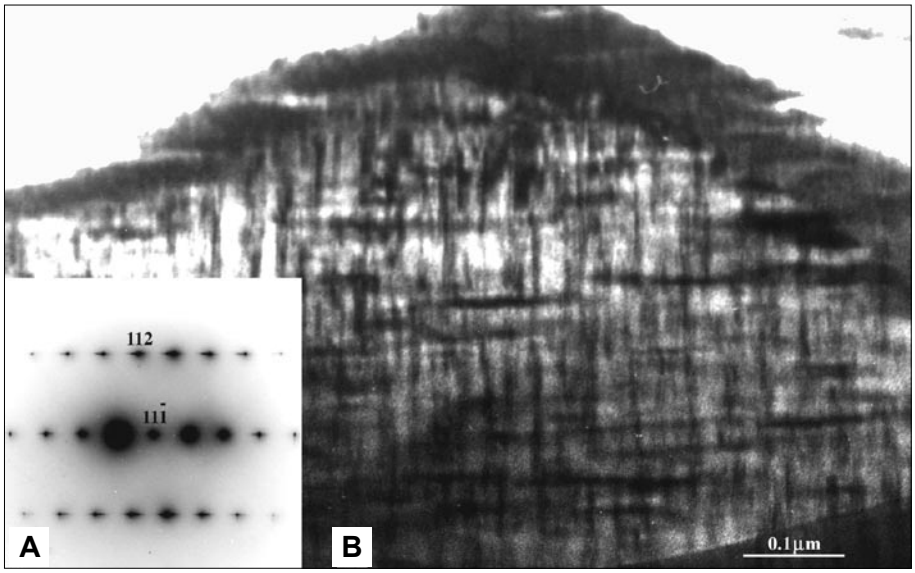

Fig. 6 <1$\bar{1}$0> zone (A) SAED pattern of Pakra Creek sample with the (B) bright field image. Note the double reflections on the diffraction pattern. Corresponding contrasts in two directions are visible on the bright field image.

of the albite patches in the Pakra Creek sample support epitaxially oriented intergrowths of these two substances. This type of intergrowth is not observable in the Sloboština Creek sample, which contains randomly distributed albite patches. This strongly suggests simultaneous crystallisation of albite and potassic feldspar by heterogeneous nucleation.

The two-feldspar geothermometer of STORMER (1975) provides solid evidence for the low temperature formation of the megacrysts. The albite content (in mole %) of coexisting plagioclase and potassic feldspars in the two megacrysts is 99%, 6% and 99%, 5%, respectively. The extrapolated crystallisation temperatures are below 400ºC, which is probably an underestimated value (PARSONS & BROWN, 1984). However, these temperatures and compositions definitely exclude homogeneous crystallisation followed by exsolution processes.

The phase diagram of alkali feldspars (SMITH, 1974; modified by BROWN, 1981 – in GRIFFEN, 1992) also allows us to infer the thermal histories of the samples (Fig. 7). The sequences of ordering states and coexisting compositions for sodium and potassic feldspars reflect the paths of their formation. The average composition of the samples, deduced from modal and EPMA data (Table 1), are marked by arrows in Fig. 7.

In the case of the Pakra Creek sample the sodium content requires perthitic exsolution and microcline twinning except precipitation below approximately 460ºC. If homogeneous nucleation occurred, the mini-

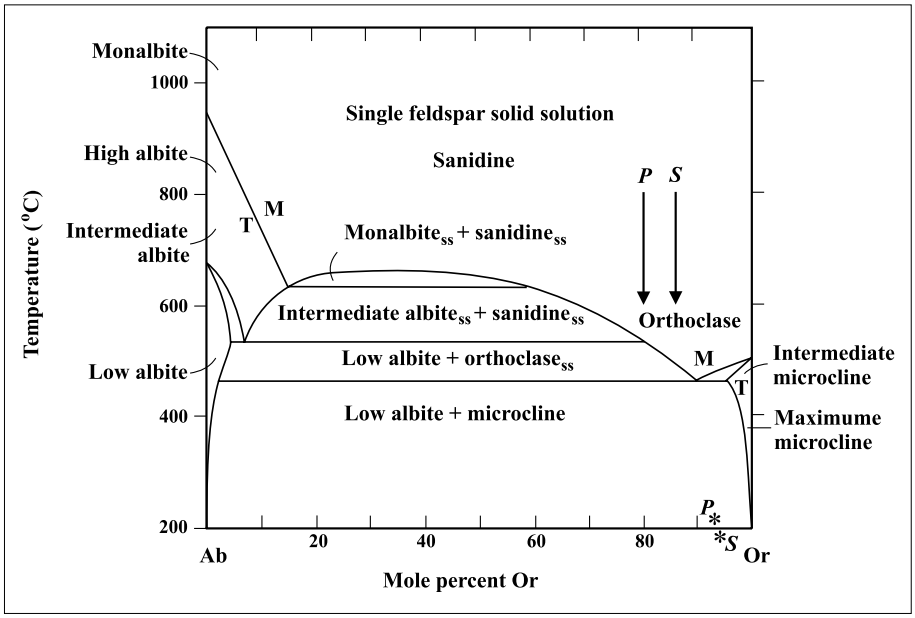

Fig. 7 Estimated average composition of the starting material (arrows) and the chemical composition of the potassic feldspar component of the megacrysts (asterisks) are shown on the phase diagram of alkali feldspars (after SMITH, 1974; modified by BROWN, 1981; in GRIFFEN, 1992). Abbreviations: P – Pakra, S – Sloboština Creek sample; M – monoclinic; T – triclinic symmetry; ss – solid solution.

mal temperature of precipitation, the actual composition, and the ordering state would be around 530ºC and orthoclase, respectively. The observed maximum microcline state has a field in the phase diagram below 460ºC. The streaks in SAED patterns and the fine scale modulations in TEM images reveal the locally inhomogeneous ordering, i.e. inhomogeneous triclinicity. This is the consequence of kinetically controlled, slow ordering at low temperature. Based on the lack of perthitic exsolution and microcline twinning, heterogeneous nucleation below 460ºC seems to be evident.

However, a slightly different origin can be concluded for the Sloboština Creek sample based on the composition (Fig. 7) and the presence of cross-hatched extinction pattern (Fig. 2B). Although there are some uncertainties regarding the origin of the cross-hatched extinction pattern (AKIZUKI, 1972; for summary see McLAREN, 1984), it is usually considered as the manifestation of the microcline twinning, which is known to be the result of orthoclase–microcline solid-state transformation (LAVES, 1950; McLAREN, 1984). SALJE et al. (1985) concluded that in triclinic Na-feldspar domains only albite and pericline twin walls are created by spontaneous strain.

The Sloboština Creek sample has a near eutectic composition ($Or_{90}Ab_{10}$). The lack of perthitic exsolution and the cross-hatched pattern observed under polarizing microscope without twinned SAED patterns suggests a precipitation temperature near to 460ºC at eutectic composition. Under these conditions, the alkali feldspar precipitated from fluids as orthoclase, and during further cooling the monoclinic orthoclase transformed to the triclinic phase characterised as intermediate microcline. This is in agreement with the two-feldspar thermometer and the resulting crystallisation temperature can be read as the lowest limit for precipitation of 460ºC. The estimated temperatures for the formation of the megacrysts allow impeded transformations to the maximum microcline state.

TEM studies revealed that both samples are continuously modulated along their (010) (Figs. 4 and 5) and ($11\bar{1}$) planes (Fig. 6). Modulations cause streaked reflections and a fine-scaled wavy contrast in TEM images. These modulations are interpreted as traces of Al/Si ordering, resulting in increasing triclinicity between intermediate and maximum microcline. It is called a tweed-like contrast system contrary to the real tweed texture, which arises from a fine pattern of microdomains with a high degree of intradomain order, but small overall degree of order (BRATKOVSKY et al., 1996). Like the spinodal decomposition which resulted in chemical inhomogenities, the triclinicity (and the unit cell parameters) varies in our structurally modulated samples on a submicron scale.

5. CONCLUSION

Both the vein filling and pocket forming occurrences, forming by segregation of a melt would require eutectic composition and texture for the $KAlSi_3O_8$–SiO_2–$NaAlSi_3O_8$ system. The solid phase segregation of the quartz component from the eutectic system produces a vermicular or spherical texture as a function of undercooling (BAKER & FREDA, 2001). The lack of graphic, vermicular or spherical textures and nonperthitic appearence of albite in the microcline host, exclude the formation of megacrysts from a melt. The textural relationship of albite and microcline, and the chemical compositions of the coexisting phases, revealed heterogeneous nucleation at low temperatures. The average value of triclinicity is high for both samples, and the inhomogeneous Al/Si ordering is reflected by fine scale variations of the cell parameters. The monoclinic orthoclase precipitated slightly above (Sloboština Creek), and below (Pakra Creek) 460ºC, transforms to microcline not by twinning, but by a spatially continuous structural modulation.

Acknowledgements

The authors acknowledge Ekhard SALJE and Vladimir BERMANEC for their helpful review, comments and suggestions. Special thanks go to Stjepan ŠĆAVNIČAR, Professor Emeritus, for his useful corrections. We are also indebted to Livia RUDNYÁNSZKY for her technical help and emotional support.

6. REFERENCES

AKIZUKI, M. (1972): Electron-microscopic investigation of microcline twinning.– Am. Min. 57, 797–808.

BAKER, D.R. & FREDA, C. (2001): Eutectic crystallization in the undercooled Orthoclase–Quartz–H_2O system: experiments and simulations.– Eur. J. Min. 13, 453–466.

BLASI, A., BRAJKOVIC, A., De POL BLASI, C., FOORD, E.E., MARTIN, R.F. & ZANAZZI, P.F. (1984): Structure refinement and genetic aspects of a microcline overgrowth on amazonite from Pikes Peak batolith, Colorado, USA.– Bull. Miner. 197, 411–422.

BERNDT, M. (1995): ICSD database.– Gmelin Institute, Karlsruhe.

BRATKOVSKY, A.M., HEINE, V. & SALJE, E.K.H. (1996): Strain effects, particularly in phase transitions.– Phil. Trans. R. Soc. Lond. A., 354, 2875–2896.

BROWN, I.D. (1981): The bond valence method: An empirical approach to chemical structure and bonding.– In: O'KEEFE, M. & NAVROTSKY, A. (eds.): Structure and Bonding in Crystals, Vol. 2. Academic Press, New York, 357 p.

BROWN, W.L. (1984): Feldspars and Feldspathoids.– NATO ASI series, ser C., 137, 541 p.

BROWN, W.L. & PARSONS, I. (1988): Zoned ternary feldspars in the Klokken intrusion: exsolution microtextures and mechanisms.– Contrib. Min. Petr., 98, 444–454.

CATHELINEAU, M. (1986): The hydrothermal alkali metasomatism effects on granitic rocks: quartz dissolution and related subsolidus changes.– J. Petr., 27, 945–965.

DEER, W.A., HOWIE, R.A. & ZUSSMAN, J. (2001): Rock-forming minerals. Framework silicates: Feldspars, Vol. 4A.– 2nd ed., Geol. Soc., London, 972 p.

EGGLETON, R.A. & BUSECK, P.R. (1980): The orthoclase–microcline inversion: a high resolution transmission electron microscope study and strain analysis. Contrib. Min. Petr., 74, 123–133.

GOLDSCHMIDT, J.R. & LAVES, F. (1954): The microcline–sanidine stability relations.– Geochim. Cosmochim. Acta, 5, 1–19.

GRIFFEN, D.T. (1992): Silicate Crystal Chemistry.– Oxford Univ. Press, Oxford, 442 p.

HAYNES, J.W. (1994): The Ordovician Deiske and Midbrig K-bentonite beds of the Cincinnati Arch and the Southern Valley and Ridge Province.– Geol. Soc. America, Spec. Pap., 290, 80 p.

JAMIČIĆ, D. (1989): Osnovna geološka karta SFRJ, 1: 100.000, List Daruvar, L 33–95 (Basic Geological Map of SFRJ 1:100000, Daruvar sheet).– Geol. zavod Zagreb (1975–1988), Savezni geološki zavod Beograd, Beograd.

JAMIČIĆ, D. (2001): Osnovne geološke značajke Slavonskih planina s osvrtom na Našičko područje [*Basic geological characteristics of the Slavonian Mts. with special regards to the Našice area* – in Croatian].– Matica Hrvatska, Našički zbornik, 6, 29–36.

JAMIČIĆ, D. & BRKIĆ, M. (1987): Osnovna geološka karta SFRJ, 1:100.000, List Orahovica, L 33–96 (Basic Geological Map of SFRJ, 1:100000, Orahovica sheet).– Geol. zavod Zagreb (1971–1986), Savezni geološki zavod Beograd, Beograd.

KOROLIJA, B. & JAMIČIĆ, D. (1989): Osnovna geološka karta SFRJ, 1:100.000, List Našice, L 34–95 (Basic Geological Map of SFRJ, 1:100000, Našice sheet).– Geol. zavod Zagreb (1988), Savezni geološki zavod Beograd, Beograd.

KROLL, H. & RIBBE, P.H. (1983): Lattice parameters, composition and Al, Si order in alkali feldspars.– In: RIBBE, P.H. (ed.): Feldspar Mineralogy. 2nd ed., Reviews in Mineralogy, 2, 57–99.

KUČAN, F. & KRMPOTIĆ, M. (1911): Mikroklinmikropertit iz Pakre [*Microclinemicroperthite from Pakra* – in Croatian].– Glasnik hrvatskog prirodoslovnog društva. Godište XXIII, Zagreb.

LAVES, F. (1950): The lattice and twinning of microcline and other potash feldspar.– Jour. Geol., 58, 548–571.

LOVAS, Gy., HORVAT, M. & BUDA, Gy. (1999): K-feldspars of the granitoids, pegmatites and migmatites from Papuk Polymetamorphic Complex in East Slavonia, Croatia.– Berichte der Deutschen Mineralogischen Gesellschaft, No.1., Beihefte zum European Journal of Mineralogy, 11, Stuttgart, p. 149.

McCONNELL, J.D.C. (1969): Electron optical study of incipient exsolution and inversion phenomena in the system $NaAlSi_3O_8$–$KAlSi_3O_8$.– Phil. Mag., 19, 221–229.

McCONNELL, J.D.C., De VITA, A., KENNY, S.D. & HEINE, V. (1997): Determination of the origin and magnitude of Al/Si ordering enthalpy in framework aluminosilicates from ab initio calculations.– Phys. Chem. Minerals, 25, 15–23.

McLAREN, A.C. (1984): Transmission electron microscope investigations of the microstructures of microclines.– In: BROWN, W.L. (ed.): Feldspars and Feldspathoids. NATO ASI series, ser C. 137, 373–409.

NEVES, L.J.P.F. & GODINHO, M.M. (1995): Estimação expedita do ordenamento Al–Si do feldspato potássico – uma reapreciação [*Expeditious estimation of Al–Si ordering in potassic feldspar – re-evaluation* – in Portuguese].– Memórias e Notícias, Publ. Dep. Ciências da Terra e do Mus. Lab. Mineral. Geol. Univ. Coimbra, 120, 15–24.

NEVES, L.J.P.F. & GODINHO, M.M. (1999): Structural state of K-feldspar in some Hercynian granites from Iberia: a review of data and controlling factors.– Can. Min., 37, 691–700.

PAMIĆ, J. & LANPHERE, M. (1991): Hercynian granites and metamorphic rocks from the Mts. Papuk, Psunj, Krndija and the surrounding basement of the Pannonian Basin in Slavonija (Northern Croatia, Yugoslavia).– Geologija, 34, 81–253, Ljubljana.

PAMIĆ, J., LANPHERE, M. & BELAK, M. (1996): Hercynian I-type and S-type granitoids from the Slavonian Mountains (southern Pannonian Basin, northern Croatia).– N. Jb. Miner. Abh., 171/2, 155–186.

PARSONS, I. & BROWN, W.L. (1984): Feldspars and the thermal history of igneous rocks.– In: BROWN, W.L. (ed.): Feldspars and Feldspathoids. NATO ASI series, ser C. 137, 317–371.

RIBBE, P.H. (1983): Aluminum–silicon order in feldspars; domain textures and diffraction patterns.– In: RIBBE, P.H. (ed.): Feldspar mineralogy. 2nd ed., Rev. in Min., 2, 21–55.

SALJE, E. & KUSCHOLKE, B. (1984): On the structural phase transitions in alkali feldspars.– Bull. Min., 107, p. 539.

SALJE, E., KUSCHOLKE, B. & WRUCK, B. (1985): Domain wall formation in minerals. 1. Theory of twin boundary shapes in Na-feldspar.– Phys. Chem. Min., 12, 132–140.

SMITH, J.V. (1974): Feldspar Minerals. I. Crystal Structure and Physical Properties.– Springer-Verlag, Heidelberg, 627 p.

SMITH, J.V. & BROWN, W.L. (1988): Feldspar Minerals. Crystal Structures, Physical, Chemical and Microtextural Properties. Vol. 1.– 2nd ed. Springer, New York.

STORMER, J.C. Jr. (1975): A practical two feldspar geothermometer.– Am. Min., 60, 667–674.

ŠIKIĆ, K. (1995): Prikaz geološke građe Medvednice [*A Review of a geological structure of the Medvednica Mt.* – in Croatian].– In: ŠIKIĆ, K. (ed.): Geološki vodič Medvednice, 7–30, Institut za geološka istraživanja INA-Industrija nafte d.d. – Naftaplin, Zagreb.

TAJDER, M. (1957): Petrografsko istraživanje zapadnog dijela Papuka [*Petrographic investigation of the western part of the Papuk Mt.* – in Croatian].– Ljetopis JAZU, 62, 316–323.

TIBBALS, J.E. & OLSEN, A. (1977): An electron microscope study of some twinning and exsolution textures in microcline amazonites.– Phys. Chem. Minerals, 1, 313–324.

WHITE, J.C. & BARNETT, R.L. (1990): Microstructural signatures and glide twins in microcline, Hemlo, Ontario.– Can. Min., 28/4, 757–769.

WILLAIME, C., BROWN, W.L. & GANDAIS, G. (1976): Physical aspects of exsolution in natural alkali feldspars.– In: WENK, H.R. (ed.): Electron Microscopy in Mineralogy. Springer-Verlag, Berlin, 248–257.

VRAGOVIĆ, M. (1965): Graniti i gnajsi Papuka [*Granites and gneisses of the Papuk Mountain* – in Croatian].– Unpubl. PhD Thesis, University of Zagreb, 222 p.

XU, H., VEBLEN, D.R., BUSECK, P. & RAMAKRISHNA, B.L. (2000): TEM and SFM of exsolution and twinning in an alkali feldspar.– Am. Min., 85, 509–514.

Manuscript received March 04, 2004.

Revised manuscript accepted November 08, 2004.